

Angular and polarization properties of a photonic crystal slab mirror

Virginie Lousse^{1,2}, Wonjoo Suh¹, Onur Kilic¹, Sora Kim¹, Olav Solgaard¹, and Shanhui Fan¹

¹Department of Electrical Engineering, Stanford University, Stanford, California 94305, USA

²Facultés Universitaires Notre-Dame de la Paix, Rue de Bruxelles 61, B-5000 Namur, Belgium
vlousse@stanford.edu

Abstract: It was recently demonstrated that a photonic crystal slab can function as a mirror for externally incident light along a normal direction with near-complete reflectivity over a broad wavelength range. We analyze the angular and polarization properties of such photonic crystal slab mirror, and show such reflectivity occurs over a sizable angular range for both polarizations. We also show that such mirror can be designed to reflect one polarization completely, while allowing 100% transmission for the other polarization, thus behaving as a polarization splitter with a complete contrast. The theoretical analysis is validated by comparing with experimental measurements.

© 2004 Optical Society of America

OCIS codes: (260.5740) Resonance; (230.0230) Optical devices; (230.4040) Mirrors; (230.5440) Polarization-sensitive devices.

References and links

1. S. Peng and G. M. Morris, "Experimental demonstration of resonant anomalies in diffraction from two-dimensional gratings," *Opt. Lett.* **21**, 549-551 (1996).
2. Wonjoo Suh, M. F. Yanik, Olav Solgaard, and Shanhui Fan, "Displacement-sensitive photonic crystal structures based on guided resonance in photonic crystal slabs," *Appl. Phys. Lett.* **82**, 1999-2001 (2003).
3. R. Magnusson and S. S. Wang, "New principle for optical filters," *Appl. Phys. Lett.* **61**, 1022-1024 (1991).
4. M. Kaskar, P. Paddon, V. Pacradouni, R. Morin, A. Busch, Jeff F. Young, S.R. Johnson, Jim MacKenzie, and T. Tiedje, "Observation of leaky slab modes in an air-bridged semiconductor waveguide with a two-dimensional photonic lattice," *Appl. Phys. Lett.* **70**, 1438-1440 (1997).
5. Shanhui Fan and J. D. Joannopoulos, "Analysis of guided resonances in photonic crystal slabs," *Phys. Rev. B* **65**, 235112 1-8 (2002).
6. S. Noda, M. Yokoyama, M. Imada, A. Chutinan, and M. Mochizuki, "Polarization Mode Control of Two-Dimensional Photonic Crystal Laser by Unit Cell Structure Design," *Science* **293**, 1123-1125 (2001).
7. Shanhui Fan, Wonjoo Suh, and J.D. Joannopoulos, "Temporal coupled-mode theory for the Fano resonance in optical resonators," *J. Opt. Soc. Am. A* **20**, 569-572 (2003).
8. V. Lousse and J.P. Vigneron, "Use of Fano resonances for bistable optical transfer through photonic-crystal films," *Phys. Rev. B* **69** (2004) (to be published).
9. J.B. Pendry and A. MacKinnon, "Calculation of photon dispersion relations," *Phys. Rev. Lett.* **69**, 2772 - 2775 (1992).
10. Wonjoo Suh and Shanhui Fan, "Mechanically switchable photonic crystal filter with either all-pass transmission or flat-top reflection characteristics," *Opt. Lett.* **28**, 1763-1765 (2003).
11. H. Sunnerud, M. Karlsson, C. Xie, and P. A. Andrekson, "Polarization-Mode Dispersion in High-Speed Fiber-Optic Transmission Systems," *J. Lightwave Technol.* **20**, 12 (2002).

1. Introduction

Dielectric optical mirrors play an essential role in wide ranges of optical devices such as filters, sensors, switches, and lasers. High-reflectivity dielectric mirrors are generally constructed using multi-layer films. A strong reflection for externally incident light has also been observed with guided resonance in 1-D or 2-D grating structures. Most experiments on

grating structures, however, showed an extremely narrow reflection peak [1]. It has been recently shown by W. Suh *et al.* [2] that broad-band near 100% reflection for normally incident light can be obtained by the use of a single dielectric layer of photonic crystal slab. The structure consists of a square lattice of air holes in a high-dielectric film. The operating mechanism of the proposed structure relies on the guided resonance phenomenon [3-6]. Such resonances are strongly confined within the slab, and the periodic index contrast provides the phase matching mechanisms that allow these modes to couple into radiation modes and possess a finite lifetime. In the vicinity of the resonance frequency, a Fano interference occurs that allows incident light to be completely reflected [7]. The resonance frequency and the lifetime of the guided resonance are determined by the structure of the photonic crystal, which provides great flexibility for engineering the optical properties.

The photonic crystal slab mirror, which consists of only a single dielectric layer, is far more compact than traditional multi-layer film structures. In addition, such a structure represents an attractive application of photonic crystal structures, as the structure functions with a relatively large optical aperture, and does not suffer from the insertion loss problems that often limit the practical use of 2-D photonic crystal waveguides.

In the present paper, we consider the angular dependency and polarization sensitivity of such a highly reflective two-dimensional photonic crystal slab. Analyzing the angular dependency is of importance for practical applications since the lateral dimensions of an incident beam are always finite and thus such beam consists of multiple angular components. We show that nearly-complete reflection can be obtained for wide frequency and incident angle ranges by the proper design of the crystal. Also, through the analysis of the polarization properties of such photonic crystal slab mirrors, we show that large polarizations selectivity can be accomplished in a straightforward fashion by using air holes with a lower symmetry. Such large polarization-selectivity is generally difficult to obtain using traditional multilayer film structures. And thus the results further indicate the potentials of photonic crystal slab mirror structures. We validate our theoretical analysis by experimentally demonstrating the mirror operations of photonic crystal slabs.

2. Angular and polarization dependence of a photonic crystal slab mirror

We consider a photonic crystal slab with a square lattice of air holes (Fig. 1). The structure has a lattice constant a . The slab has a dielectric constant $\epsilon = 12$, a thickness $h = 0.55a$, and cylindrical air holes with a radius of $R = 0.4a$. It has been shown that a broadband reflection at normal incidence of over 99% reflection can be accomplished [2]. From an experimental point of view, however, an incident beam with a finite cross-section contains multiple angular components. A realistic description of a photonic crystal slab mirror should therefore take into account the incidence-angle dependence of the transfer function. For a photonic crystal slab mirror, the incidence direction is specified by two polar angles, the colatitude angle θ (angle from the normal direction), and the azimuthal angle ϕ . These angles are schematically shown in Fig. 1. We apply light in the form of plane waves at various incidences to the photonic crystal structure and detect the total transmitted power as a function of the angles θ and ϕ .

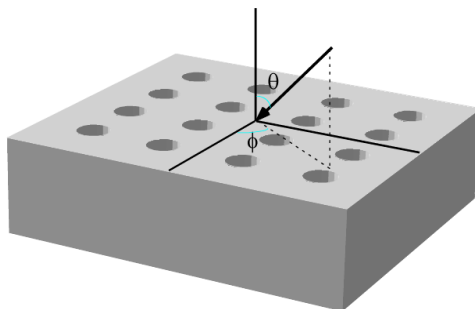


Fig. 1. Photonic crystal structure consisting of a square lattice of circular air holes in a dielectric slab.

The calculations were done with the transfer-matrix method in a momentum-space representation [8]. In this approach, the film is discretized along the propagation direction into small segments. The T-matrix (i.e., the transfer matrix, which relates the wave amplitudes from one side of the film to the other side) for each segment is then determined directly from the Maxwell's equations. In principle, all these T-matrices can be multiplied to produce the T-matrix of the whole film from which the transmission and reflection coefficients of the film can be determined. However, it is known that direct cascading of the T-matrix leads to numerical instability. Instead, here we overcome the numerical instability by converting the T-matrix to the S-matrix (i.e., the scattering matrix, which relates the outgoing waves to the incoming waves) for each segment, and by cascading these S-matrices together [9]. In doing so, for each segment, we express the electric and magnetic fields in the incoming waves and outgoing waves in a plane wave basis with the wavevectors determined by the Bloch theorem, and retain the coefficients for only the lowest n_g reciprocal lattice vectors in the two-dimensional lattice. For each reciprocal lattice vector, we retain the plane waves with both polarizations, as well as the incoming and outgoing waves. This representation thus contains the full polarization and angular information, so that all incidence angles can be treated.

The advantage of this formalism is that it allows the whole range of incidence angles θ to be dealt with in an efficient way. The results of the calculations are shown on Fig. 2, where the transmission is represented as a function of the normalized frequency va/c (vertical axis) and the incidence angle θ (horizontal axis). Three different values of the angle ϕ (given in degrees) were plotted: $\phi = 0$ (Fig. 2(a)), $\phi = 25$ (Fig. 2(b)) and $\phi = 45$ (Fig. 2(c)). For each of them, the two incident polarizations were separately studied. The TE (transverse electric) incident polarization has an electric field normal to the incidence plane, while the TM (transverse magnetic) incident polarization has a magnetic field normal to the incident plane. For an arbitrary incidence direction, these polarizations are not conserved in the outgoing waves. Here, we are concerned only with total power in the outgoing wave.

At normal incidence ($\theta = 0$), we observe two very high-reflectivity regions, and in particular a broad frequency zone of near complete reflectivity located around the frequency $0.532 c/a$. The transmission curve obtained with the transfer matrix with 64 (8x8) plane waves in this case agrees with the one obtained with the FDTD method (finite-difference time-domain method) [2], except for a small blue shift. This shift is explained by the slow convergence of our lateral plane wave expansion, which tends to slightly modify the model dielectric constant at the hole lateral edges. Better agreements were obtained with 256 (16x16) plane waves. The calculations with 64 plane waves, however, capture all the essential features of the transmission spectra. Below we will use the results with 64 plane waves.

The angular polarization plots in Fig. 2 show that the broad strong-reflectivity remains for a wide range of incidence angles θ . For both polarizations, the reflectivity in this frequency range stays higher than 95 % when the angle θ is increased from 0° to 15° . For higher incidence angles, transmission peaks due to additional resonances progressively appear in the high-reflectivity window, first for the TE polarization, and then, for both polarizations. The high-reflectance zones therefore close at high angles partly due the presence of lower-order resonances.

At normal incidence, in addition to the high-reflectivity zone at $0.532c/a$, an additional zone of high reflectivity is found at a lower frequency of $0.471c/a$. These two high-reflectivity regions correspond to totally different modal patterns (Fig. 3). The broad high-reflectance zone arises from a TE-like resonance with an electric field parallel to the slab (Fig. 3(b)). On the other hand, the lower resonance corresponds to a TM-like resonance, with a higher quality factor and thus a longer lifetime and a smaller bandwidth (Fig. 3(a)). Thus, the presence of air holes provides a much stronger scattering for the TE waves compared with the TM waves.

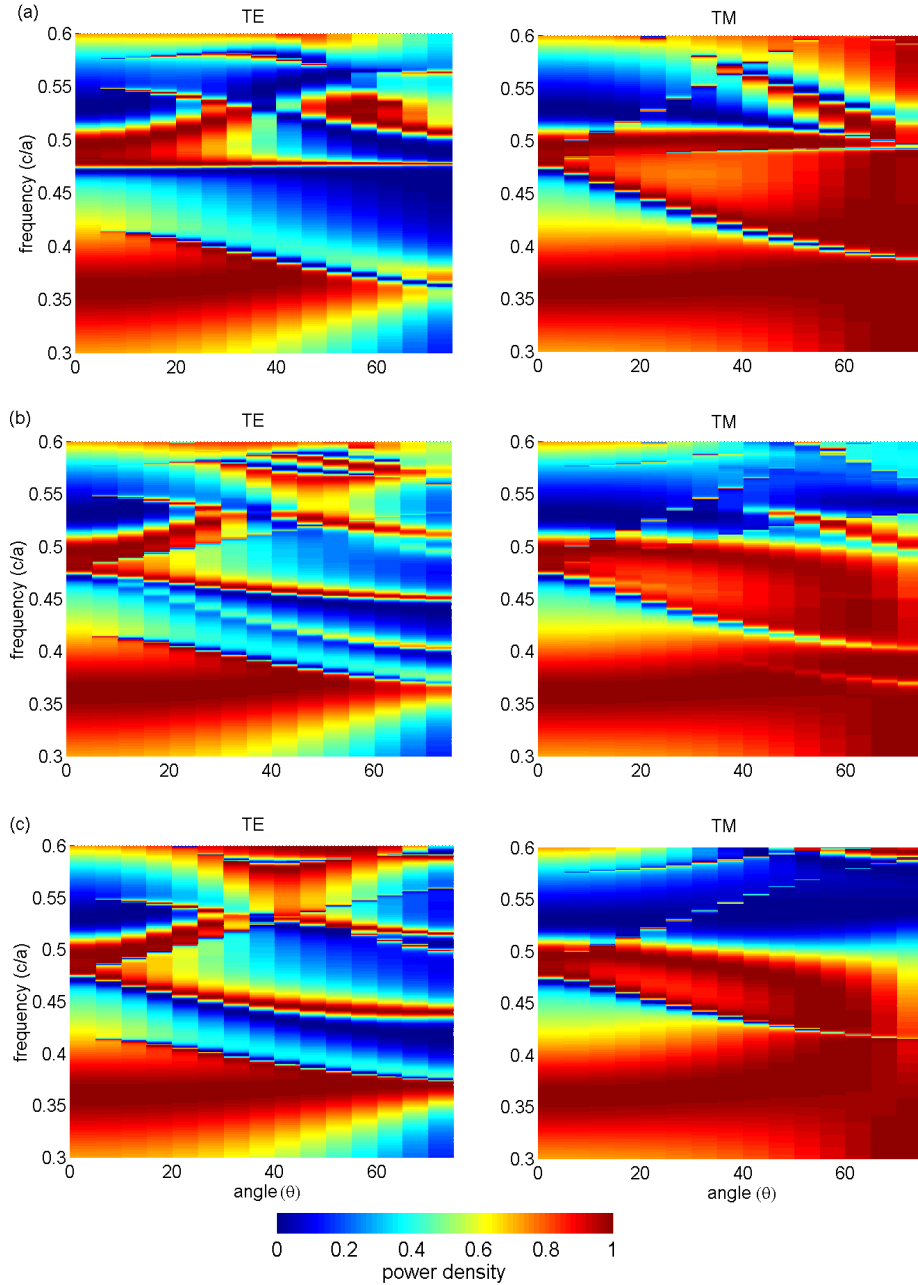


Fig. 2. Angular study of the filter responses for the photonic crystal structure in Fig. 1. Three different values of the angle ϕ (given in degrees) were considered: $\phi = 0$ (Fig 2(a)), $\phi = 25$ (Fig 2(b)) and $\phi = 45$ (Fig 2(c)). For each of them, both possible incident polarizations were separately studied. The panels on the left are related to an incident TE-polarization, while those on the right correspond to the TM-polarization.

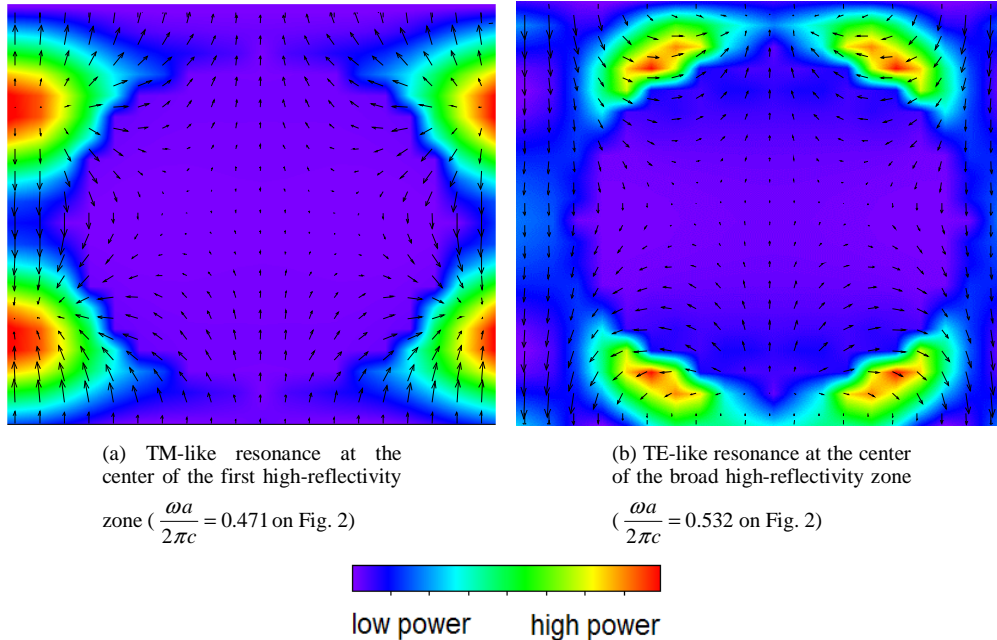


Fig. 3. Color plots for the intensity of a single unit cell of the photonic crystal slab of Fig. 1. The center of the plots corresponds to the center of the cylindrical air hole in the unit cell, and the incidence considered here is normal. Within the figures, the vector plots of the in-plane electric field are superimposed.

3. Polarization-dependent mirror

The ability to control the transmission spectrum by varying the radius of air holes and the thickness of the slab in the photonic crystal makes it possible to design reflectors or filters for specific applications. In the example considered in the previous section, at normal incidence direction, there is a 90-degree rotational symmetry, and therefore the reflectivity is independent of the polarization. On the other hand, when the rotational symmetry of the structure is reduced, one could create mirrors that are polarization dependent. One simple way to proceed is to use rectangular holes as shown in Fig. 4(a). We choose the thickness of the slab such that the background transmission at the operating frequency is unity. Also, we choose the size of the rectangular air holes to create a resonance for only one polarization at the operating frequency. In particular, when we use a rectangular hole with dimensions of $0.4a$ in the x -direction and $0.2a$ in the y -direction, in a slab with a thickness of $h = 0.55a$ and a dielectric constant of 12, the spectral function at normal incidence is such that the x -polarized light has 100% transmission while the y -polarized light is completely reflected in a Lorentzian line shape, as shown in Fig. 4(b). This selective behavior illustrates the potentials and flexibilities of photonic crystal slab structures. It would have been quite challenging to construct such a strongly polarization dependent mirror with multi-layer dielectric films.

Such a mirror can be important for polarization control in vertical surface emitting lasers. One could further create devices geometries by cascading multiple slabs. For example, it has been shown in Ref. [10] that an all-pass filter can be created by cascading two slabs together. Such an all-pass filter generates 100% transmission both on- and off-resonance while creating a strong on-resonance delay. With the polarization properties of the slab proposed here, by cascading two slabs together, it is then possible to let both polarizations pass through, while significantly delaying one polarization versus the other. This filter function could be very interesting in mitigation of polarization mode dispersion [11].

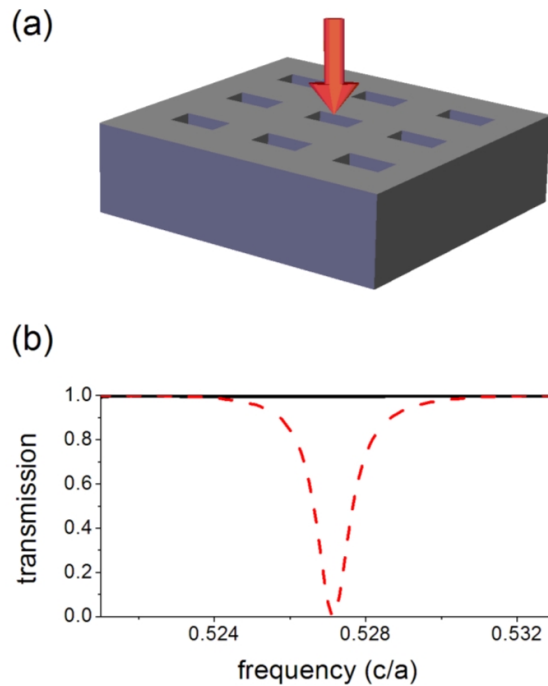


Fig. 4. (a) Photonic crystal slab structure with rectangular air holes for generating anisotropic spectral response. (b) Transmission spectrum upon normally incident light, through the photonic crystal slab represented on Fig 4(a). These calculations were done with the FDTD method. The x -polarized light (solid line) has 100% transmission while the y -polarized light (dotted red line) is completely reflected in a Lorentzian line shape.

4. Experimental results

We validate the theoretical prediction of a broadband reflection of a photonic crystal slab by comparing it with experiments. A suspended photonic crystal structure was fabricated in a silicon slab with a thickness of 340 nm. An array of holes with a radius of 330 nm, arranged on a simple square lattice with a periodicity of 998 nm was introduced into the slab as shown in Fig. 5(a). The transmission spectra were determined by normalizing the measured transmitted power through the slab with respect to the power reaching the spectrum analyzer when there was no sample in the setup. We reproducibly observe strong transmission extinction with an average of 20 db in the range 1220-1255 nm. Spectra measured on different, but nominally identical, crystals only showed minor variations. We also verified that the spectra taken at normal incidence were polarization insensitive by rotating a polarizer in front of the PC sample.

The measured transmission is compared with FDTD simulations in Fig. 5(b). The simulations, carried out for a normal-incident plane wave on an infinite array of holes ($a = 998$ nm, $R = 0.37a$, $h = 0.335a$, $\epsilon = 11.7$), are in excellent agreement with the measured data. In particular, both theory and experiments confirm the existence of strong and broadband reflectivity from a single photonic crystal slab.

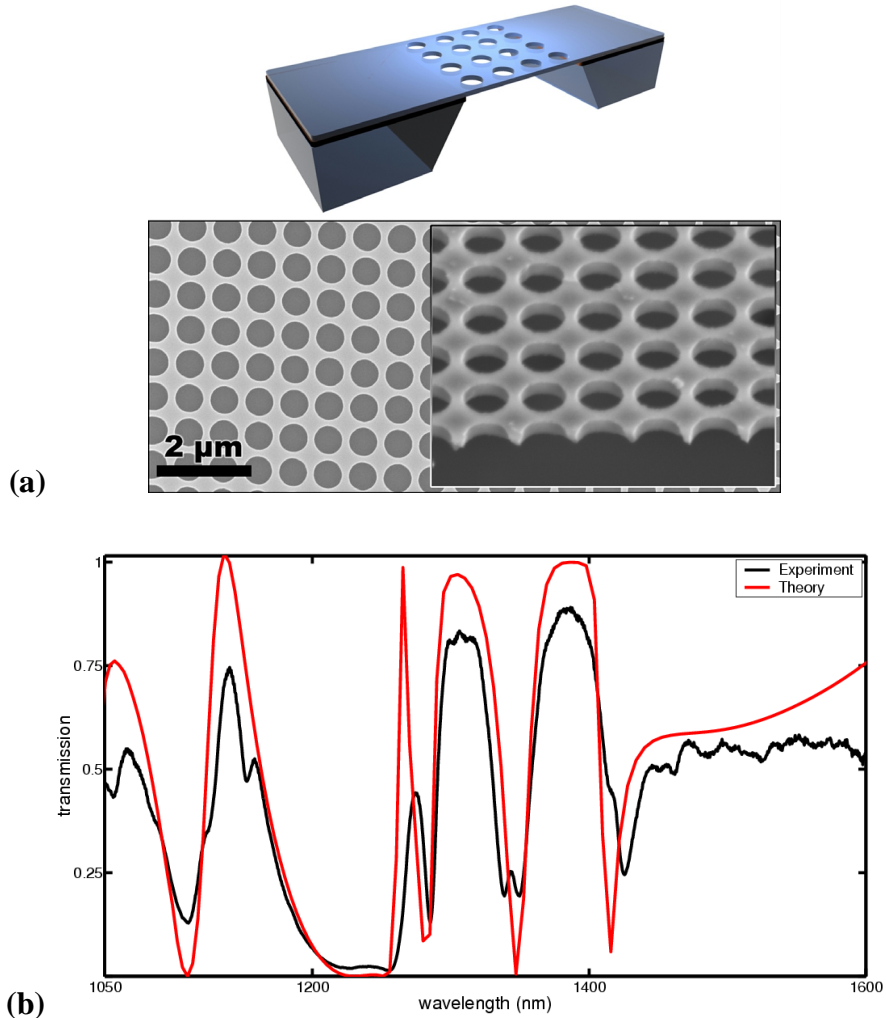


Fig. 5. (a) Fabricated photonic crystal silicon structure. (b) The experimental transmission spectrum is compared with FDTD simulations for a normally incident light with an infinite beam size.

5. Conclusion

We have considered a highly reflective structure built from a two-dimensional photonic crystal film and described its dependence on the incidence direction and on the incident wave polarization. This demonstrated the use of guided resonances to provide complete reflectivity with a wide angular range. Furthermore, we showed that this system can provide a polarization selective optical response by simply breaking the rotational symmetry. Our approach deviates from the more standard practice of the use of a multilayer film, with which the reflectance is created by constructive interference of multiple reflections on a large number of accurately deposited interfaces. With a planar multilayer stack, strong reflectivity will occur only in structures with sufficiently large number of layers (typically on the order of 10 to 100). By contrast, the photonic crystal slab uses material and lateral geometry parameters to adjust the reflectance values within a single dielectric layer. The device is more compact and may be more easily fabricated, with a shortened growth cycle and a high degree of perfection with modern lithography techniques. Compared to multilayers, the photonic

crystal slab also provides a greater flexibility for controlling the polarization dependence of the reflectance. The compactness of the structure further facilitates the mechanical tuning of such structures when two slabs are assembled in parallel pairs, which are potentially important for displacement sensing, optical switching and dispersion control [2,10].

Acknowledgments

The simulations were made possible through grants from the NSF National Resource Allocation Committee (NRAC), and the IBM-SUR program. Funding for this work was provided in part by Army Research Laboratories under grant DAAD-17-02-C-0101, and by Canon Development America through the Center for Integrated Systems at Stanford University. V.L. was supported as a Research Fellow by the Belgian National Fund for Scientific Research (FNRS) and by a Fellowship of the Belgian American Educational Foundation.